Technical Report No. 32-613

Microwave Spectrum, Barrier to Internal Rotation, and Quadrupole Coupling Constants of Cis-1-Chloropropylene

Robert A. Beaudet

JET PROPULSION LABORATORY

CALIFORNIA INSTITUTE OF TECHNOLOGY

PASADENA, CALIFORNIA

May 1, 1964

Microwave Spectrum, Barrier to Internal Rotation, and Quadrupole Coupling Constants of *Cis*-1-Chloropropylene*

Robert A. Beaudet†

Mallinckrodt Chemical Laboratory, Harvard University, Cambridge, Massachusetts

and

Jet Propulsion Laboratory, California Institute of Technology, Pasadena, California

$2940\,4$

The microwave spectrum of $CH_3CH = CH^{35}Cl$ and $CH_3CH = CH^{37}Cl$ was studied in the region from 8–35 kMc/sec. The height of the potential barrier hindering the internal rotation of the methyl top is 620 cal/mole; the Cl quadrupole coupling constants are $\chi_{aa}{}^{35Cl} = -19.66$ Mc/sec and $\chi_{bb}{}^{35Cl} = 31.05$. The dipole moments are $\mu_a = 1.47$ D and $\mu_b = 0.72$ D. The even greater lowering of the barrier, *trans* to *cis*, for the chlorine compounds as compared with the fluorine analogs supports the hypothesis of a nonbonded interaction between the halogen and the methyl hydrogen atoms.

anth.

I. INTRODUCTION

THE study of the microwave spectrum of the fluoropropylenes has revealed that *cis*-$CH_3CH = CHF$ has an abnormally low potential barrier hindering the rotation of the methyl group about the C–C single bond. While the barrier height V_3 in $CH_3CH = CH_2$,[1] *trans*-$CH_3CH = CHF$,[2] and $CH_3CF = CH_2$[3] varies from 2.0 to 2.4 kcal/mole, V_3 is lowered to 1.0 kcal/mole in *cis*-$CH_3CH = CHF$,[4] presumably by a nonbonded interaction between the fluorine atom and the methyl hydrogens.

As can be seen in Fig. 1, since the van der Waals[5] radii overlap to a larger extent in *cis*-$CH_3CH = CHCl$, we would expect an even stronger interaction in this case than in the corresponding fluorine compound.

The microwave spectrum of *cis*-$CH_3CH = CHCl$ has been studied in the region from 8–35 kMc/sec. From the splittings of the rotational transitions a barrier height of 620 cal/mole has been found. This barrier height has been confirmed from the first-order Stark splitting of the E component of the $3_{12} \leftarrow 2_{11}$ transition. The quadrupole coupling constants of ^{35}Cl were obtained from the hyperfine splittings due to the coupling of the quadrupole moment of the Cl nucleus with the surrounding electric field.

II. EXPERIMENTAL

A sample of *cis*- and *trans*-chloropropylene was purchased from the Columbia Organic Chemical Company, Columbia, South Carolina. The *cis* isomer was isolated by vapor-phase chromatography. A Perkin–Elmer chromatograph equipped with a 6-ft "R" column was

† National Science Foundation Fellow, 1957–1961. Present address: Department of Chemistry, University of Southern California, University Park, Los Angeles, California.

[1] D. R. Lide, Jr., and D. E. Mann, J. Chem. Phys. **27**, 868 (1957).

[2] S. Siegel, J. Chem. Phys. **27**, 989 (1957).

[3] L. Pierce and J. M. O'Reilly, J. Mol. Spectry. **3**, 536 (1959).

[4] R. A. Beaudet and E. B. Wilson, Jr., J. Chem. Phys. **37**, 1133 (1962).

[5] L. Pauling, *The Nature of the Chemical Bond* (Cornell University Press, Ithaca, New York, 1960), p. 260.

adequate to obtain 95% separation. The cis-CH₃CH=CHCl did not isomerize even when it was stored at room temperature, but the sample was normally kept at liquid-nitrogen temperatures. The compound was sufficiently volatile that its microwave spectrum could be studied at dry-ice temperatures.

A conventional 100-kc/sec. Stark-modulated microwave spectrometer was used. This instrument has previously been described in detail.[6,7] The frequencies were measured by comparing the microwave signals with multiples of a 32-Mc/sec oscillator which was phase-locked to a 1.0-Mc/sec signal from a Hewlett-packard Model 104A frequency standard. The standard was periodically monitored with WWV.

III. OBSERVED SPECTRUM AND ASSIGNMENT

The observed spectrum of cis-CH₃CH=CHCl is dense with nearly continuous background of weak lines in many regions. The barrier to internal rotation splits the transitions into doublets whose members (A and E) are widely separated. The E members often display a first-order Stark effect which splits the ±M degeneracy. Only the lines of A symmetry could be fitted to a rigid-rotor Hamiltonian. The transitions are further split by the interaction of the quadrupole moment of the Cl nucleus with the surrounding electric field gradient.

As can be deduced from Fig. 2, a- and b-type selection rules apply. Since the b dipole moment is one-third as large as the a moment, the b-type lines should be approximately one-tenth as intense as the a-type lines.

The a-type transitions were identified by their quadrupole splittings and their characteristic Stark effects. The lines were strong and were measured to an accuracy of about ±0.05 Mc/sec when the hyperfine structure was completely resolved. Once B_A and C_A were determined from the a spectra, A was estimated from the relation

$$I_a = I_c + \Delta' - I_b,$$

where Δ' was assumed to be about 3.0 amu-Å².

The b-type spectrum of only the ³⁵Cl isotopic species could be assigned. The spectrum was weak and had to be observed with relatively high pressures in the absorption cell (≈ 30–$40\,\mu$). Due to only partial Stark modulation even the higher J Q-branch transitions were weak. The spectrum was assigned by making trial $\Delta E(\kappa)$ versus $(A-C)$ plots, and was confirmed by the quadrupole splitting patterns. Because the b spectrum of the ³⁷Cl isotope is only one third as intense as that of the ³⁵Cl, the lines of the former should only have a signal to noise ratio of 1–2. Hence, it is understandable that the b spectrum of this species was not assigned. The measured A-level lines are given in Table I.

The E levels were usually assigned by their quadrupole splittings. It was assumed that the quadrupole pattern was the same for the A and E members of the

internal rotation doublets. For some transitions the A–E splittings are very large (≈ 100 Mc/sec) and the E member has a first-order Stark effect. Since these lines were easily broadened by imperfect zero basing of the square wave, their intensities were reduced and the quadrupole splittings could not always be resolved. Hence some E levels could not be conclusively assigned. The measured A–E splittings are given in Table II.

As will be seen in Sec. V, the A levels can be fitted to rigid-rotor formulas except for small corrections due to the fourth-order and D perturbation terms. For the low J transitions, the fourth-order terms are negligible, but the D terms have effects of the order of 1 Mc/sec. The rotational constants A_A, B_A, and C_A for CH³⁵CH=CH³⁵Cl were determined from the frequencies of the $2_{11} \leftarrow 1_{10}$, $2_{12} \leftarrow 1_{11}$, and $1_{11} \leftarrow 0_{00}$ transitions. The observed frequencies of the lines are first corrected for nuclear quadrupole coupling effects and the small higher-order internal rotation effects. The corrected frequencies are then simple linear combinations of A_A, B_A, and C_A. The "true" rotational constants of the rigid rotor were then obtained from the relationships

$$A_A = A + F\alpha^2 W_{0A}^{(2)},$$

$$B_A = B + F\beta^2 W_{0A}^{(2)},$$

$$C_A = C.$$

Both the observed and the "true" rotational constants are given in Table III.

IV. MOMENTS OF INERTIA AND STRUCTURE

The moments of inertia were obtained from the "true" rotational constants. Because CH₃CH=CHCl has a plane of symmetry with only the two hydrogens of the methyl group out of this plane, the relation $I_a + I_b - I_c = I_\alpha - \Delta$ will hold. I_α is the moment of inertia of the methyl top about its axis of symmetry, Δ is the inertial defect of the planar atoms and limits the precision with which the coordinates can be determined. If I_α is assumed to be 3.104 amu-Å², Δ becomes 0.124 amu-Å². The small value of Δ is in agreement with the hypothesis of a planar structure for CH₃CH=CHCl except for the two methyl hydrogen atoms.

Only the B_A and C_A rotational constants could be accurately determined for CH₃CH=CH³⁷Cl since the a-type spectrum is insensitive to A_A. B_A and C_A were obtained from the $3_{12} \leftarrow 2_{11}$ and $3_{13} \leftarrow 2_{12}$ transitions after corrections were made for the effects of quadrupole coupling, internal rotation, and centrifugal distortion, which were assumed to be the same as in the ³⁵Cl species. The final moments of inertia for both species are given in Table III.

Because only two isotopic species were studied, a complete structure determination could not be carried out; however, by assuming that the structural parameters are the same as in CH₃CH=CH₂ which has been

[6] R. L. Poynter, Rev. Sci. Instr. **34**, 77 (1963).
[7] R. L. Poynter, (to be published).

TABLE I. Observed transitions in CH₃CH=CH³⁵Cl and CH₃CH=CH³⁷Cl.

Part I. CH₃CH=CH³⁵Cl

a-type transitions[a]:

$J \leftarrow J'$	$F \leftarrow F'$	ν_A(obs.)	ν_A(calc.)	Deviation
$2_{02} \leftarrow 1_{01}$	5/2←5/2 ⎱ 3/2←1/2 ⎰	13 135.84	13 135.98	−0.11
	7/2←5/2 ⎱ 5/2←3/2 1/2←1/2 ⎰	13 141.13	13 141.23	−0.10
	3/2←1/2 ⎱ 3/2←3/2 ⎰	13 144.73	13 144.64	+0.09
$2_{12} \leftarrow 1_{11}$	5/2←5/2	12 473.84±0.3	12 473.15	0.69
	5/2←3/2	12 475.95	12 475.99	−0.04
	3/2←1/2	12 476.52	12 476.41	0.11
	7/2←5/2	12 480.90	12 480.91	−0.01
	3/2←3/2	b	12 481.54	...
	1/2←1/2	12 484.40±0.2	12 484.17	0.23
$2_{11} \leftarrow 1_{10}$	3/2←3/2	13 862.20	13 862.24	−0.04
	5/2←3/2	13 864.28	13 864.27	0.01
	3/2←1/2	13 869.16	13 869.19	−0.03
	5/2←5/2	13 871.88	13 872.04	−0.16
	1/2←1/2	13 873.54	13 873.36	0.18
	3/2←1/2	13 876.22	13 876.21	0.01
$3_{03} \leftarrow 2_{02}$	5/2←3/2	19 627.14	19 627.54	−0.40
	3/2←1/2	19 627.64	19 628.03	−0.39
	5/2←5/2	19 628.35	19 628.61	−0.26
	7/2←7/2	19 628.76	19 629.10	−0.34
$3_{13} \leftarrow 2_{12}$	5/2←3/2 ⎱ 7/2←5/2 ⎰	18 696.53	18 696.82 ⎱ 18 698.11 ⎰	−0.29
	3/2←1/2 ⎱ 9/2←7/2 ⎰	18 697.86	18 698.19 ⎱ 18 699.48 ⎰	−0.29
		18 699.15		−0.33
$3_{12} \leftarrow 2_{11}$	7/2←5/2 ⎱ 5/2←3/2 ⎰	20 780.20	20 780.32 ⎱ 20 781.67 ⎰	−0.12
	9/2←7/2 ⎱ 3/2←1/2 ⎰	20 781.66	20 781.70 ⎱ 20 783.05 ⎰	−0.02
		20 782.91		−0.19
$3_{22} \leftarrow 2_{21}$	7/2←5/2	19 757.14	19 757.19	−0.05
	5/2←3/2	19 760.64	19 760.70	−0.06
	9/2←7/2	19 762.10	19 762.10	−0.00
	3/2←1/2	19 765.64	19 765.61	+0.03
$3_{21} \leftarrow 2_{20}$	7/2←5/2	19 889.31	19 889.57	−0.26
	5/2←3/2	19 892.82	19 892.93	−0.11
	9/2←7/2	19 893.87	19 893.99	−0.12
	3/2←1/2	19 897.26	19 897.33	−0.07

$J \leftarrow J'$	$F \leftarrow F'$	ν_A(obs.)	ν_A(calc.)	Deviation
$4_{04} \leftarrow 3_{03}$	11/2←9/2	26 019.89	26 020.03	−0.14
	9/2←7/2 ⎱ 7/2←5/2 ⎰	26 020.45	26 020.47 ⎱ 26 020.56 ⎰	−0.05
	5/2←3/2	b	26 021.10	...
$4_{14} \leftarrow 3_{13}$	7/2←5/2	24 893.66	24 894.13 ⎱ 24 894.78 ⎰	−0.47
	5/2←3/2 ⎱ 9/2←7/2 ⎰	24 894.44	24 894.97	−0.44
	11/2←9/2	24 895.16	24 895.61	−0.45
$4_{23} \leftarrow 3_{22}$	9/2←7/2	26 320.20	26 320.45	−0.25
	7/2←5/2	26 320.94	26 321.19	−0.25
	11/2←9/2	26 322.29	26 322.55	−0.26
	5/2←3/2	26 322.97	26 323.29	−0.32
$4_{22} \leftarrow 3_{21}$	9/2←7/2	26 647.43	26 647.88	−0.45
	7/2←5/2	26 647.87	26 648.49	−0.62
	11/2←9/2	26 648.82	26 649.35	−0.53
	5/2←3/2	26 649.32	26 649.96	−0.64
$5_{05} \leftarrow 4_{04}$	9/2←7/2 ⎱ 11/2←9/2 ⎰	32 291.96	32 292.81 ⎱ 32 293.03 ⎰	−1.05
	7/2←5/2 ⎱ 13/2←11/2 ⎰	32 292.70	32 293.56 ⎱ 32 293.78 ⎰	−0.97
$5_{15} \leftarrow 4_{14}$	9/2←7/2	31 061.70	31 062.55	−0.85
	11/2←9/2	31 062.20	31 062.98 ⎱ 31 063.10 ⎰	−0.84
	7/2←5/2 ⎱ 13/2←11/2 ⎰	31 062.64	31 063.53	−0.89
$5_{14} \leftarrow 4_{13}$	11/2← 9/2 9/2← 7/2 13/2←11/2 7/2← 5/2	34 514.30±0.4	34 514.97 34 515.16 34 515.45 34 515.64	... ...
$5_{24} \leftarrow 4_{23}$	11/2←9/2 ⎱ 9/2←7/2 ⎰	32 859.45	32 860.16 ⎱ 32 860.34 ⎰	−0.80
	13/2←11/2 ⎱ 7/2←5/2 ⎰	32 860.55	32 861.28 ⎱ 32 861.46 ⎰	−0.82
$5_{23} \leftarrow 4_{22}$	11/2←9/2 ⎱ 9/2←7/2 ⎰	33 500.74	33 501.58 ⎱ 33 501.64 ⎰	−1.17
	13/2←11/2 ⎱ 7/2←5/2 ⎰	33 501.09	33 501.84 ⎱ 33 502.01 ⎰	−0.83
$5_{33} \leftarrow 4_{32}$	11/2←9/2	33 036.46	33 036.79	−0.33
	9/2←7/2	33 037.21	33 037.54	−0.33
	13/2←11/2	33 038.59	33 038.85	−0.26
	7/2←5/2	33 039.29±0.2	33 039.70	−0.41

TABLE I (Continued)

Part I. CH₃CH=CH³⁶Cl

a-type transitions*: (Continued)

$J \leftarrow J'$	$F \leftarrow F'$	ν_A(obs.)	ν_A(calc.)	Deviation
$5_{32} \leftarrow 4_{31}$	11/2←9/2	33 057.09	33 057.51	−0.42
	9/2←7/2	33 057.74	33 058.24	−0.50
	13/2←11/2	33 059.14	33 059.62	−0.48
	7/2←5/2	33 059.81	33 060.36	−0.53
$5_{41} \leftarrow 5_{40}$ $5_{42} \leftarrow 5_{41}$	11/2←9/2	33 005.62	33 006.42	−0.80
	9/2←7/2	33 007.10	33 007.97	−0.87
	13/2←11/2	33 009.37	33 010.21	−0.84
	7/2←5/2	33 010.91±0.3	33 011.76	−0.85
b-type transitions				
$1_{11} \leftarrow 0_{00}$	5/2←3/2	17 145.41	17 145.50	−0.09
	3/2←3/2	17 148.37	17 148.36	0.01
$2_{12} \leftarrow 1_{01}$	5/2←3/2	23 038.65	23 038.51	0.14
	7/2←5/2	23 041.40	23 041.35	0.05
	3/2←3/2	23 044.18	23 044.05	0.13
$5_{05} \leftarrow 4_{14}$	7/2←5/2	24 446.00	24 447.39	−1.39
	13/2←11/2	24 447.44	24 448.80	−1.36
	9/2←7/2	24 448.60	24 450.04	−1.44
	11/2←9/2	24 449.97	24 451.47	−1.50
$4_{13} \leftarrow 4_{04}$	5/2←5/2	14 777.80	14 777.48	+0.32
	11/2←11/2	14 780.21	14 779.99	+0.22
	7/2←7/2	14 785.15	14 784.65	+0.50
	9/2←9/2	14 787.55	14 787.17	+0.38
$5_{14} \leftarrow 5_{05}$	7/2←7/2	16 999.52	16 999.58	−0.06
	13/2←13/2	17 001.71	17 001.68	+0.03
	9/2←9/2	17 007.03	17 007.02	+0.01
	11/2←11/2	17 008.93	17 009.16	−0.23
$6_{15} \leftarrow 6_{06}$	9/2←9/2	19 874.31	19 874.64	−0.33
	15/2←15/2	19 876.16	19 876.49	−0.33
	11/2←11/2	19 882.05	19 882.46	−0.31
	13/2←13/2	19 883.93	19 884.31	−0.38
$7_{16} \leftarrow 7_{07}$	11/2←11/2	23 456.21	23 457.53	−1.32
	17/2←17/2	23 457.88	23 459.20	−1.32
	13/2←13/2	23 464.37	23 465.72	−1.35
	15/2←15/2	23 466.81	23 467.39	−1.58
$8_{17} \leftarrow 8_{08}$	13/2←13/2	27 757.34	27 760.17	−2.83
	19/2←19/2	27 758.83	27 761.68	−2.85
	15/2←15/2	27 765.78	27 768.64	−2.86
	17/2←17/2	27 767.26	27 770.15	−2.89

b-type transitions[d] (Continued)

$J \leftarrow J'$	$F \leftarrow F'$	ν_A(obs.)	ν_A(calc.)	Deviation
$4_{25} \leftarrow 4_{13}$	9/2←9/2	29 808.22	29 807.42	+0.54
	7/2←7/2		29 807.94	
	11/2←11/2	29 809.20	29 808.89	+0.07
	5/2←5/2		29 809.39	
$5_{23} \leftarrow 5_{14}$	11/2←11/2	28 794.84	28 794.07	+0.58
	9/2←9/2		28 794.45	
	13/2←13/2	28 796.11	28 795.40	+0.62
	7/2←7/2		28 795.78	
$6_{24} \leftarrow 6_{15}$	13/2←13/2	27 940.58	27 939.35	1.13
	11/2←11/2		27 939.54	
	15/2←15/2	27 941.28	27 940.15	1.03
	9/2←9/2		27 940.34	
$7_{26} \leftarrow 7_{16}$	15/2←15/2	27 399.80±0.30	27 398.95	+0.80
	13/2←13/2		27 398.97	
	17/2←17/2		27 399.02	
	11/2←11/2		27 399.03	
$8_{26} \leftarrow 8_{17}$	13/2←13/2	27 313.85	27 312.59	1.20
	19/2←19/2		27 312.72	
	15/2←15/2	27 314.62	27 313.34	1.21
	17/2←17/2		27 313.48	
$9_{27} \leftarrow 9_{18}$	15/2←15/2	27 804.02	27 802.34	1.56
	21/2←21/2		27 802.59	
	17/2←17/2	27 805.63	27 803.94	1.57
	19/2←19/2		27 804.20	
$10_{2,8} \leftarrow 10_{1,9}$	17/2←17/2	28 969.33	28 970.15	0.97
	23/2←23/2		28 970.50	
	19/2←19/2	28 971.80	28 972.58	0.95
	21/2←21/2		28 972.92	
$11_{2,9} \leftarrow 11_{2,10}$	19/2←19/2	30 889.84	30 893.49	3.65
	25/2←25/2	30 890.28	30 893.91	3.63
	21/2←21/2	30 893.04	30 896.70	3.66
	23/2←23/2	30 893.47	30 897.12	3.65
$12_{2,10} \leftarrow 12_{1,11}$	21/2←21/2	33 626.08	33 633.98	7.90
	27/2←27/2	33 626.54	33 634.45	7.91
	23/2←23/2	33 629.78	33 637.91	8.13
	25/2←25/2	33 630.40	33 638.39	7.99

TABLE I (*Continued*)

Part II. CH₃CH=CH³⁷Cl

$J \leftarrow J'$	$F \leftarrow F'$	ν_A(obs.)	ν_A(calc.)	Deviation
$2_{02} \leftarrow 1_{01}$	7/2←5/2, 5/2←3/2	12 863±0.3	12 863.95	−0.06
$2_{11} \leftarrow 1_{10}$	5/2←3/2	13 559.20±0.3	13 559.14	0.06
	7/2←5/2	13 563.36±0.3	13 563.01	0.35
$2_{12} \leftarrow 1_{11}$	7/2←5/2	12 227.21±0.5	12 226.98	0.23
$3_{03} \leftarrow 2_{02}$	c	19 219.23±0.5	14 219.50	−0.27
$3_{13} \leftarrow 2_{12}$	5/2←3/2	18 318.20	18 318.44	−0.24
	7/2←5/2	18 319.29	18 319.45	−0.19
	3/2←1/2		18 319.52	
	9/2←7/2	18 320.40	18 320.55	−0.25
$3_{12} \leftarrow 2_{11}$	7/2←5/2	20 323.23	20 323.30	−0.07
	5/2←3/2	20 324.35	{ 20 325.36	−0.02
	9/2←7/2		20 325.38 }	
	3/2←1/2	20 325.27	20 326.45	−0.18
$4_{04} \leftarrow 3_{03}$	c	25 484.81±0.3	25 486.86	−2.05
$4_{14} \leftarrow 3_{13}$	c	24 392.05±0.5	24 392.90	−0.85
$4_{13} \leftarrow 3_{12}$	c	27 060.70±0.5	27 061.16	−0.46
$4_{23} \leftarrow 3_{22}$	9/2←7/2	25 763.14	25 763.33	−0.19
	7/2←5/2	25 763.68	25 763.91	−0.23
	11/2←9/2	25 764.81	25 764.98	−0.17
	5/2←3/2	25 765.33	25 765.56	−0.23

$J \leftarrow J'$	$F \leftarrow F'$	ν_A(obs.)	ν_A(calc.)	Deviation
$4_{22} \leftarrow 3_{21}$	9/2←7/2	26 066.18	26 064.86	+1.31
	7/2←5/2	26 066.54	26 065.32	1.22
	11/2←9/2	26 067.22	26 066.01	1.21
	5/2←3/2	26 067.62	26 066.49	1.13
$5_{05} \leftarrow 4_{04}$	11/2←9/2	31 639.74	31 643.04	−3.40
	9/2←7/2		31 643.21	
	7/2←5/2		31 643.61	−3.40
	13/2←11/2	31 640.30	31 643.78	
$5_{15} \leftarrow 4_{10}$	c	30 438.37	30 439.61	−1.24
$5_{14} \leftarrow 4_{13}$	c	33 761.74	33 763.26	−1.52
$5_{24} \leftarrow 4_{23}$	11/2←9/2	32 166.06	32 166.86	−0.93
	9/2←7/2		32 167.00	
	13/2←11/2	32 166.98	32 167.74	−0.83
	7/2←5/2		32 167.88	
$5_{23} \leftarrow 4_{22}$	c	32 760.75	32 758.90	+2.15
$5_{33} \leftarrow 4_{32}$	11/2←9/2	32 330.08	32 330.04	0.04
	9/2←7/2	32 330.82	32 330.63	0.19
	13/2←11/2	32 332.00	32 331.74	0.26
	7/2←5/2	32 332.45	32 332.33	0.12
$5_{32} \leftarrow 4_{31}$	11/2←9/2	32 346.28	32 348.37	−1.99
	9/2←7/2	32 347.32	32 348.85	−1.73
	13/2←11/2	32 348.62	32 349.94	−1.32
	7/2←5/2	32 349.25	32 350.52	−1.27

a These frequencies were measured to ±0.05 Mc/sec unless indicated otherwise.
b Hidden under more intense line.
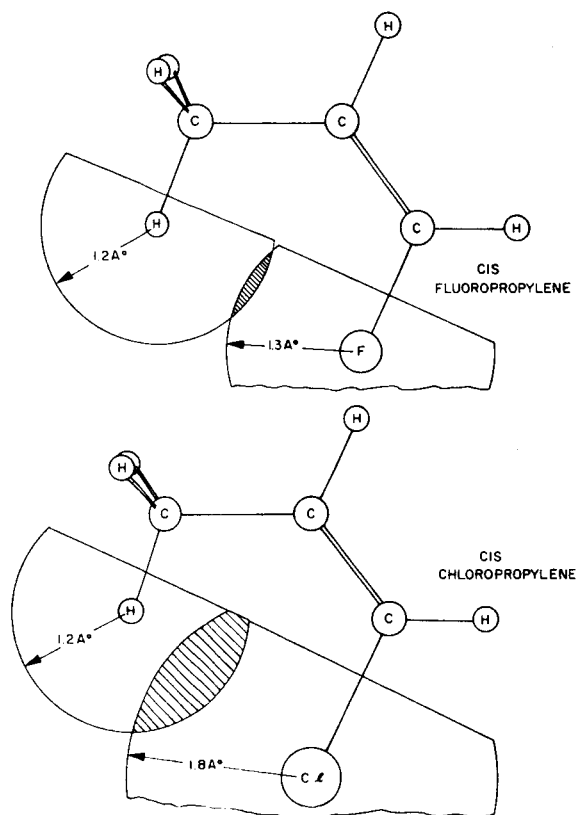c Calculated quadrupole splittings are less than 0.5 Mc/sec.

FIG. 1. Comparison of nonbonded interactions in cis-$CH_3CH=$ CHF and cis-$CH_3CH=CHCl$.

thoroughly studied by Lide and Christensen,[8a] the C–Cl bond length and bond angle could be fitted to the moments of inertia. The results are given in Table IV.

Since it is unlikely that the C–Cl bond length should change from 1.728 Å in vinyl chloride[8b] to 1.738 in cis-1-chloropropylene while the $\angle$ C–C$=$C remained constant, the $\angle$ C$=$C–C and $\angle$ C$=$C–Cl were varied to fit the moments of inertia. The results were $\angle$ C$=$C–C$=127.5°\pm0.2°$ and $\angle$ C–C–Cl$=123.0°\pm0.2°$.
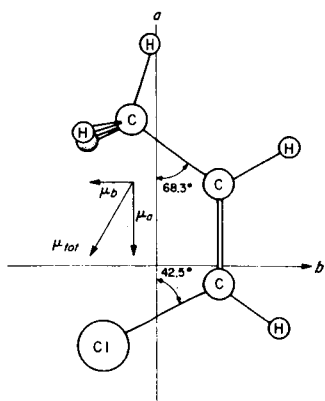

FIG. 2. Principal axes and dipole moment of cis-$CH_3CH=CHCl$.

[8] (a) D. R. Lide, Jr. and D. Christensen, J. Chem. Phys. **35**, 1374 (1961). (b) D. Kivelson, E. B. Wilson, Jr., and D. R. Lide, Jr., *ibid.* **32**, 205 (1960).

V. QUADRUPOLE COUPLING CONSTANTS

The hyperfine structure of the $CH_3CH=CHCl$ rotational transitions is accounted for by first-order quadrupole coupling effects. The quadrupole splittings of

TABLE II. Internal rotation splittings.

Part I. $CH_3CH=CH^{35}Cl$.

$J \leftarrow J'$	$(\nu_A - \nu_B)_{obs}$	V_3
$2_{02} \leftarrow 1_{01}$	10.91 Mc/sec	618 cal/mole
$3_{03} \leftarrow 2_{02}$	14.43	619
$3_{13} \leftarrow 2_{12}$	<0.5	⋯
$3_{12} \leftarrow 2_{11}$	26.23	620
$4_{04} \leftarrow 3_{03}$	16.50	617
$4_{14} \leftarrow 3_{13}$	6.65	599[a]
$4_{13} \leftarrow 3_{12}$	28.30	620
$4_{23} \leftarrow 3_{22}$	−78.81	638
$4_{22} \leftarrow 3_{21}$	117.98	628
$5_{05} \leftarrow 4_{04}$	16.96	614
$5_{15} \leftarrow 4_{14}$	9.77	591[a]
$5_{14} \leftarrow 4_{13}$	33.90	618
$5_{24} \leftarrow 4_{23}$	−61.58	634
$5_{23} \leftarrow 4_{22}$	111.57	626
$5_{14} \leftarrow 5_{05}$	34.30	623
$6_{15} \leftarrow 6_{06}$	57.52	626
$7_{16} \leftarrow 7_{07}$	86.68	629
$8_{17} \leftarrow 8_{08}$	120.86	630
$6_{24} \leftarrow 6_{15}$	−43.93	624
$7_{25} \leftarrow 7_{16}$	−22.55	620
$8_{26} \leftarrow 8_{17}$	−5.23	627
$9_{27} \leftarrow 9_{1,8}$	12.36	640
$10_{2,8} \leftarrow 10_{1,9}$	35.12	591
$11_{2,9} \leftarrow 11_{1,10}$	65.08	617

Part II. $CH_3CH=CH^{37}Cl$

$J \leftarrow J'$	$(\nu_A - \nu_B)_{obs}$	V_3
$2_{02} \leftarrow 1_{01}$	10.33	626
$3_{03} \leftarrow 2_{02}$	13.97	624
$3_{13} \leftarrow 2_{12}$	<0.5	⋯
$3_{12} \leftarrow 2_{11}$	25.16	628
$4_{04} \leftarrow 3_{03}$	15.73	625
$4_{14} \leftarrow 3_{13}$	7.20	a
$4_{13} \leftarrow 3_{12}$	27.52	625
$4_{23} \leftarrow 3_{22}$	75.2	656
$4_{22} \leftarrow 3_{21}$	118.4	626
$5_{05} \leftarrow 4_{04}$	16.62	617
$5_{15} \leftarrow 4_{14}$	9.53	602
$5_{14} \leftarrow 4_{13}$	32.22	626
	Average	622±9

[a] V_3 is very sensitive to small errors in these splittings.

the $J=2_{11} \leftarrow 1_{10}$ and $J=2_{12} \leftarrow 1_{11}$ transitions are independent of the molecular structure, and also are larger than the quadrupole splittings of the higher J transitions. Hence, the quadrupole coupling constants are best obtained from these low J lines. Because hyperfine components with $\Delta F=0$ and with $\Delta F=\pm1$ were

measured, all three coupling constants could be obtained.

The value of χ_{aa} which was determined from the spacing between the $F=7/2\leftarrow5/2$ and $F=5/2\leftarrow3/2$ components of both of these rotational transitions is -19.66 Mc/sec χ_{cc} which was determined independently from the separation between the $F=3/2\leftarrow1/2$ and $F=3/2\leftarrow3/2$ components and between the $F=5/2\leftarrow3/2$ and the $F=5/2\leftarrow5/2$ components of the $J=2_{11}\leftarrow1_{10}$ transitions, and from the separations between the $F=3/2\leftarrow1/2$ and the $F=1/2\leftarrow1/2$ components of the $J=2_{11}\leftarrow1_{11}$ transitions is 31.05 Mc/sec χ_{bb} was then obtained from Laplace's equation,

$$\chi_{aa}+\chi_{bb}+\chi_{cc}=0.$$

An inadequate number of hyperfine components of the $J=2\leftarrow1$ transitions of the ^{37}Cl isotopic species was seen to independently determine the quadrupole coupling constants of this isotopic form. Hence, the coupling constants were obtained from the known relation of $Q^{37}{}_{Cl}/Q^{35}{}_{Cl}$.[9] The results are given in Table V.

If the molecular parameters given in Table IV are assumed, then the angle formed by the a axis and the C–Cl bond is 47.5° (see Fig. 2). If it is further assumed that the principal axis of the quadrupole tensor lies along the C–Cl bond, then $\chi_{\alpha\alpha}$ and $\eta=(\chi_{\beta\beta}-\chi_{\gamma\gamma})/\chi_{\alpha\alpha}$ can be calculated. In this axis system α is in the direction of the C–Cl bond, β is perpendicular to the α axis, and in the plane of symmetry of the molecule, and γ is parallel to the c axis. The value of $\chi_{\alpha\alpha}$, $\chi_{\beta\beta}$, and $\chi_{\gamma\gamma}$ are given in Table III. Since $\angle a$–0–α is close to 45°, the coupling constants in the principal axis system are extremely sensitive to the exact orientation of the principal axes, and to the actual $\angle$C=C–Cl angle. A deviation of about 0.3° in $\angle a$–C–Cl would account for a change of 10 Mc/sec in $\chi_{\alpha\alpha}$. Hence, no significance can be attached to the large differences in $\chi_{\alpha\alpha}$ between *cis*- and *trans*-CH$_3$CH=CHCl ($\chi_{\alpha\alpha}$ in the *trans* isomer is -71.2 ± 2.0 Mc/sec).

TABLE III. Rotational constants of CH$_3$CH=CH^{35}Cl and CH$_3$CH=CH^{37}Cl.

	CH$_3$CH=CH^{35}Cl	CH$_3$CH=CH^{37}Cl
A_A	14 201.86 Mc/sec[a]	14 200±100 Mc/sec
B_A	3640.76	3557.67
C_A	2945.92	2889.06
A	14 194.43 Mc/sec	⋯
B	3637.76	3554.68
C	2945.92	2889.06
I_a	35.6147 amu·Å²	35.7±0.05[b] amu·Å²
I_b	138.9676	142.2156
I_c	171.6037	174.9811

[a] The rotational constants are estimated to be accurate to ±0.20 Mc/sec.
[b] Determined from the relation $I_a+I_b-I_c=I_\alpha-\Delta$.

[9] C. H. Townes and A. L. Schawlow, *Microwave Spectroscopy* (McGraw-Hill Book Company, Inc., New York, 1955), p. 644.

TABLE IV. Structure of *cis*-CH$_3$CH$_2$=CHCl.

Assumed Coordinates[a]

$r(C_1=C_2)=1.336$ Å	$\angle C_2=C_1-H=121.5°C$
$r(C_2-C_3)=1.501$	$\angle C_1=C_2-C_3=124.3°$
$r(C_1-H)=1.081$	$\angle C_1=C_2-H=119.0°$
$r(C_2-H)=1.090$	$\angle C_3-C_2-H=116.7°$
$r(C_3-H)=1.090$	$\angle H_m-C-H_m=107.7°$

Fitted Coordinates

	CH$_3$CH=CH^{35}Cl	CH$_3$CH=CH^{37}Cl
r(C—Cl)	1.735±0.005 Å	1.740 Å
$\angle$C=C—Cl	125.2°±0.2°	125.0°

Internal Rotation Parameters

$\lambda_a=68.0°$
$I_\alpha=3.104$ amu·Å²
$\alpha=0.03270$
$\beta=0.02074$
$F=1.6817$ Mc/sec

VI. BARRIER TO INTERNAL ROTATION

Tunneling through the threefold barrier to internal rotation can split the triply degenerated energy levels into a nondegenerate level ($\sigma=A$) and a doubly degenerate level ($\sigma=E$). The energy levels and the spectra of each type of level can be treated separately by fitting to the Hamiltonian[10]:

$$H_{v\sigma}=H_{rigid}+F\sum_{n=1}^{\infty}W_{v\sigma}{}^{(n)}\mathcal{P}^n+H_{v\sigma}{}^{(D)},$$

where

$$H_{rigid}=AP_z{}^2+BP_x{}^2+CP_y{}^2,$$

$$\alpha=\lambda_aI_\alpha/I_a, \qquad \beta=\lambda_bI_\alpha/I_b, \qquad \gamma=\lambda_cI_\alpha/I_c,$$

$$F=\hbar^2/2rI_\alpha r=1-\sum\lambda_g{}^2I_\alpha/I_g,$$

$$\mathcal{P}=\alpha P_z+\beta P_x+\gamma P_y.$$

λ_g is the direction cosine of the internal top axis with respect to the g axis, I_α is the moment of inertia of the top about its axis of rotation, and $W_{v\sigma}{}^{(n)}$ is the barrier-height-dependent perturbation coefficient defined and tabulated by Herschbach.[10]

To an accuracy sufficient to fit the low J transitions the effective Hamiltonians for the A and E levels are

$$H_{vA}=H_{vA}{}^{(2)}+H_{vA}{}^{(b)},$$

$$H_{vE}=H_{vE}{}^{(2)}+H_{vE}{}^{(a)}+H_{vE}{}^{(b)},$$

[10] For a discussion of internal rotation and definition of symbols see: D. Herschbach, J. Chem. Phys. **31**, 91 (1959); D. Herschbach, *Tables for the Internal Rotation Problem* (Department of Chemistry, Harvard University, Cambridge, Massachusetts).

TABLE V. Quadrupole coupling constants.

	Principal axis system	
	^{35}Cl	^{37}Cl[a]
χ_{aa}	-19.66 Mc/sec	-15.49 Mc/sec
χ_{bb}	31.05	24.47
χ_{cc}	-11.39	-8.98
	C–Cl bond axis system	
	^{35}Cl	
$\chi_{\alpha\alpha}$	-62.83 Mc/sec	
$\chi_{\beta\beta}$	31.76 Mc/sec	
$\chi_{\gamma\gamma}$	31.05 Mc/sec	
η	$+0.0113$	

[a] The quadrupole constants for the ^{37}Cl isotope were obtained by multiplying those for the ^{35}Cl isotope by $Q^{37}\mathrm{Cl}/Q^{35}\mathrm{Cl}$.

where

$$H_{vA}^{(2)} = A_A P_z^2 + B_A P_x^2 + C_A P_y^2,$$

$$H_{vA}^{(b)} = F W_{vA}^{(4)} \mathcal{P}^4 + H_{vA}^{(D)},$$

$$H_{vE}^{(2)} = A_E P_z^2 + B_E P_x^2 + C_E P_y^2,$$

$$H_{vE}^{(a)} = F\{W_{vE}^{(1)} \alpha P_z$$
$$+ W_{vE}^{(3)}(\alpha^3 P_z^3 + \alpha\beta^2[\{P_z, P_x^2\} + P_x P_z P_x])\},$$

$$H_{vE}^{(b)} = F\{W_{vE}^{(1)}\beta P_x + W_{vE}^{(4)} \mathcal{P}^4\} + H_{vE}^{(D)}.$$

$H_{vE}^{(D)}$ and $H_{vA}^{(D)}$ are the contributions from the D terms defined by Herschbach.[10] The quadratic terms have been combined with the rotational constants to yield apparent moments of inertia:

$$A_\sigma = A + F\alpha^2 W_{v\sigma},$$
$$\sigma = A \text{ or } E,$$
$$B_\sigma = B + F\beta^2 W_{v\sigma}.$$

Both the linear and the quadratic terms contributed significantly to the total splittings; the effect of the cubic and quartic terms was an order of magnitude smaller.

Since the $H_{vE}^{(a)}$ matrix elements coupled nearly degenerate energy levels, their effect was often very large and a perturbation treatment was not justified. Hence, the effect of these terms was obtained by directly diagonalizing the Hamiltonian

$$H' = H_{vE}^{(2)} + H_{vE}^{(a)}.$$

The terms $H_{vA}^{(b)}$ and $H_{vE}^{(b)}$ were treated by first- and second-order perturbations. The $H_v^{(D)}$ was treated by the method described by Herschbach.[10] Though the $H^{(D)}$ term does have significant effects on the energy levels, the effects are so similar for the A and E levels that this term does not contribute greatly to the $A-E$ splittings. The calculated spectra in Table I, however, contains the corrections due to the $H^{(D)}$ and the $\mathcal{P}^4$ terms.

An independent determination of the barrier height can be obtained from each $A-E$ splitting. The expected splitting for each transition was plotted as a function of $s = 4V_3/9F$ at intervals of $s = 0.2$. The parameters which were used are given in Table IV. A value of the barrier was then obtained from each observed splitting by linear interpolation. Some transitions were found to be extremely sensitive to the parameters used in the calculation due to the near cancellation of the linear and quadratic terms. These transitions furnished values of V_3 which deviated appreciably from the mean value. The angle θ formed by the symmetry axis of the methyl top and the a principal axis was then varied between $66°-72°$ to attempt to improve the agreement of the value of V_3 determined from these sensitive transitions. However, any change in θ from the estimated value only caused further divergences in V_3. Hence, the best value of V_3 obtained with $\theta = 68°$ was 622 cal/mole with an average deviation of ± 9 cal/mole.

VII. STARK EFFECT AND DIPOLE MOMENT

The dipole moment was determined by studying the Stark effects of the A members of the $3_{02} \leftarrow 2_{02}$, $3_{12} \leftarrow 2_{11}$, and $4_{13} \leftarrow 3_{12}$ transitions. All measurements were carried out at high electric fields to eliminate the interaction of the nuclear quadrupole coupling with the Stark effect. The electric field in the absorption cell was calibrated by measuring the frequency displacements of the $J = 2 \leftarrow 1$ line of OCS at various voltage settings of the square-wave generator.

The calculated dipole moments are given in Table VI. The measured and calculated Stark effects for these transitions are also compared. Since only the absolute value of the dipole moment components along the principal axes are determined, there exists an ambiguity in the direction of the total dipole. The signs of the two components were chosen so that the total dipole was approximately parallel to the C–Cl bond. Then μ_{tot} is oriented $10°$ from the C–Cl bond direction.

Most E level lines with $K_{-1} > 0$ exhibited a first-order Stark effect which splits the $\pm |M|$ degeneracy. By measuring this splitting for the $3_{12} \leftarrow 2_{11}$ line, our value of the barrier height was confirmed.

This effect arises because the P_z term causes mixing of the eigenfunction of near degenerate asymmetry

TABLE VI. Stark effect of cis-$CH_3CH{=}CH^{35}Cl$.

Transition	$(\Delta\nu/\mathcal{E}^2)_{obs}$	$(\Delta\nu/\mathcal{E}^2)_{calc}$
$3_{03} \leftarrow 2_{02}(m=1)$	-1.607×10^{-6}	-1.604×10^{-6}
$3_{12} \leftarrow 2_{11}(m=0)$	-2.322×10^{-5}	-2.28×10^{-5}
$3_{12} \leftarrow 2_{11}(m=1)$	-6.935×10^{-5}	-6.62×10^{-5}
$4_{13} \leftarrow 3_{12}(m=2)$	-3.380×10^{-6}	-3.83×10^{-6}

$$\mu_a = 1.47 \pm 0.05 \text{ D}$$
$$\mu_b = 0.72 \pm 0.03 \text{ D}$$
$$\mu_{tot} = 1.64 \pm 0.05 \text{ D}$$

doublets. Consider the Hamiltonian

$$H = H° + H_A + DP_z - \mu_z \mathcal{E} \cos\phi_{zZ},$$

where

$$D = \alpha F W_{vE}^{(1)},$$

$$H° = (B+C)P^2/2 + [2A - (B+C)]P_z^2/2$$

is the usual symmetric-rotor Hamiltonian,

$$H_A = (B-C)(P_x^2 - P_y^2)/2$$

is the asymmetry term, and the last term is the Stark-effect term. Setting up the energy matrix in a symmetric-rotor representation, we find three types of nonzero matrix elements, denoted by $\langle J, K, M \mid J', K', M \rangle$. The first, the diagonal elements are

$$\langle J, K, M \mid J, K, M \rangle$$

$$= \tfrac{1}{2}J(J+1)(B+C) + \tfrac{1}{2}\{[2A - (B+C)]K^2\}$$

$$+ DK - \mu_z \mathcal{E}[J(J+1)]^{-1}KM.$$

The second type are the usual asymmetry terms $\langle J, K, M \mid H_A \mid J, K\pm2, M \rangle$, and the third are the usual Stark-effect elements which connect $\langle J \mid J+1 \rangle$ blocks and which will not contribute to the linear Stark-effect unless there occurs an accidental degeneracy.

For $K_{-1} = \pm1$ energy levels of any J, a general relationship for the first-order Stark-effect can easily be derived from perturbation theory. In our prolate-rotor representation, the nearly degenerate $K = \pm1$ levels are directly connected by the asymmetry term $\langle J, 1, M \mid H_A \mid J, -1, M \rangle$. All other off-diagonal terms will contribute only to higher orders in the perturbation expansion. Hence, only a 2×2 matrix

$$H^{(1)} = \begin{vmatrix} E_{sym} + D' & J(J+1)(B-C)/2 \\ J(J+1)(B-C)/2 & E_{sym} - D' \end{vmatrix}$$

has to be diagonalized for each value of M, where

$$D' = D - \mu_z \mathcal{E}[J(J+1)]^{-1}M.$$

Furthermore, it is usually convenient to expand the resulting eigenvalues in a series in terms of $D/(B-C)$ and to obtain directly only the frequency splitting between the $M = + \mid M \mid$ and $M = - \mid M \mid$ lobes. Hence,

$$v_{+m} - v_{-m} = \frac{8\mu_z \mathcal{E}MD}{B-C}\left\{\left(\frac{1}{J^2(J+1)^2} - \frac{1}{J'^2(J'+1)^2}\right)\right.$$

$$\left. - \left(\frac{1}{J^4(J+1)^4} - \frac{1}{(J'^4)(J'+1)^4}\right)\frac{8D^2}{(C-B)^2}\right\} + \cdots,$$

when $J' = J+1$ represents the higher of the two J levels. This expression has previously been used for
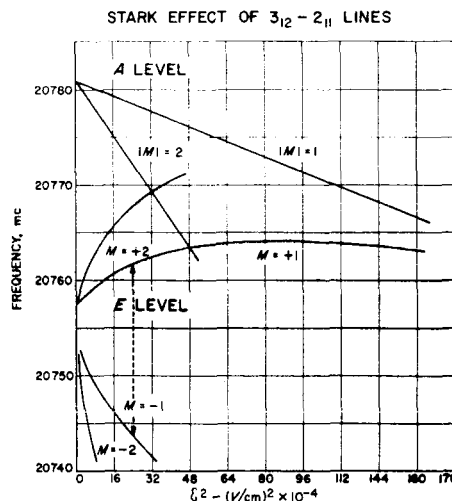

STARK EFFECT OF $3_{12} - 2_{11}$ LINES

FIG. 3. Stark effect of $J = 3_{12} - 2_{11}$ E level transition.

$J = 2\leftarrow1$ lines, where the total undiagonalized energy matrix is only a 2×2 matrix.[11]

For a $J = 3\leftarrow2, K_{-1} = 1$ transition this expression reduces to

$$v_{m=+1} - v_{m=-1} = \frac{\mu_z \mathcal{E}MD}{(B-C)}\left\{\frac{1}{6} - \frac{5}{68}\frac{D^2}{(B-C)^2}\right\}.$$

The observed Stark effect of the E level of the $J = 3_{12}\leftarrow2_{11}$ line is shown in Fig. 3. Using the value of μ_z determined from the second-order Stark effect, $D = \alpha F W_{vE}^{(1)}$ which is dependent on the barrier height V_3 can be determined. From the splittings of the $m = \pm1$ and $m = \pm2$ lobes, barrier heights of 624 cal/mole and 597 cal/mole were obtained. This compares favorably with the value of 620 cal/mole obtained from frequency splittings.
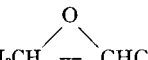
VIII. DISCUSSION

The internal rotation barrier heights decrease from 2.2 kcal/mole in *trans*- to 0.620 kcal/mole in *cis*-1-chloropropylene. This greater lowering of the barrier than observed in the fluorine analogs supports the existence of a nonbonded interaction between the halogens and the methyl hydrogens. Since the interaction distance in *cis*-1-chloropropylene is less than in *cis*-1-fluoropropylene, and since the van der Waals radius[5] of Cl is larger than that of F, the nonbonded interactions would be greater in the former.

As Beaudet and Wilson[4] have mentioned, the lowering of the barrier, *trans* to *cis*, can be explained if the interaction between the halogen and the methyl hydrogens is governed by a Morse-like potential with a steep repulsive side at short separations of H and X, and a gentle attractive slope at larger separations. There is little doubt that the stable conformation of the $-CH_3$

[11] (a) D. R. Lide, Jr., J. Chem. Phys. **27**, 343 (1957). (b) J. M. O'Reilly and L. Pierce, *ibid.* **34**, 1176 (1961).

TABLE VII. Barriers to internal rotation in the propylenes.

Compound	V_3(cal/mole)	Reference
$CH_3CH=CH_2$	1978	1
trans-$CH_3CH=CHF$	2200	2
$CH_3CF=CH_2$	2430	3
trans-$CH CH=CHCl$	2170	18
cis-$CH_3CH=CHF$	1060	4
cis-$CH_3CH=CHCN$	1400	20
cis-$CH_3CH=CHCH_3$	750	19
cis-$CH_3CH \overset{O}{\underset{}{\diagup\diagdown}} CHCH_3$	1600	23
cis-$CH_3CH=CHCl$	620	this work

group is the same as that in propylene,[12] namely, the *staggered* conformation where the methyl hydrogens are staggered with respect to the ethylenic hydrogen. Large changes in energy would be needed to account for a change in the stable conformation. When the methyl hydrogens are *eclipsed* with respect to the ethylenic hydrogen, the molecular configuration is unstable.

The large overlap of the van der Waals radii and the apparent opening of the $\angle C=C-Cl$ and $\angle C-C=C$ angles in the *cis* isomer suggests that the atomic separations are on the steep repulsive portion of the H···Cl potential curve. On the other hand, isomerization studies of the *cis* and *trans* dihaloethylenes indicate that the *cis* isomer is more stable than the *trans* isomer in CHCl=CHCl by $\Delta H_0° = 445$ cal/mole,[13] and in CHF=CHF by even more.[14]

Pitzer and Hollenberg[13] explained the additional stability of *cis* CHCl=CHCl by the larger contribution of the resonance forms
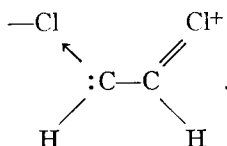
This form is stabilized in the *cis* isomers by the proximity of the positive and negative ends. This may be considered as a valence bond visualization of a nonbonded interaction.

From the hyperconjugation viewpoint similar reso-

nant structures can be drawn for the halopropylenes:

(A)   (B)
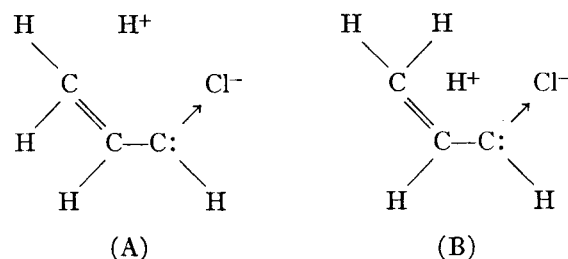
With the knowledge of $\Delta H_0°$ (*cis→trans*) and V_3 for the *cis* and *trans* isomers in 1-chloropropylene, it should be possible to estimate the contributions of A and B to the total energy.

Unfortunately, very little data exists on the isomerization of halopropylenes: for 1-chloropropylene,[15] $K_{isom} = [cis]/[trans] \simeq 1.5$, and for bromopropylene[16] $K_{isom} = 4.0$ in the gas phase. This data is insufficient to calculate $\Delta H_0°$ for these compounds. Hence, the more stable isomer cannot be determined.

The thermal *cis–trans* isomerization of crotononitrile, $CH_3CH=CHCN$, has been studied.[17] In this compound, $\Delta H_0°$ (*trans→cis*) = -0.170 ± 0.12 kcal/mole and the barrier V_3 is lowered from over 2.3 kcal in the *trans* isomer to 1.4 kcal, in the *cis* isomer. The barrier height of the *cis* isomer, V_3 (*cis*), can be expressed as a function of V_3 (*trans*), the additional interaction energy of the *cis* isomer in the *staggered* conformation, ΔH (*cis*, staggered), and ΔH (*cis*, eclipsed) the additional interaction energy of the *cis* isomer in the *eclipsed* conformation. Then

$$\Delta V_3 = V_3(cis) - V_3(trans) = \Delta H(cis, \text{ eclipsed})$$
$$- \Delta H(cis, \text{ staggered}) = -800 \text{ cal/mole.} \quad (1)$$

Assuming that the staggered form is more stable, and that the steric repulsions between the methyl hydrogens and the chlorine are negligible in the eclipsed configuration, then

$$\Delta H(cis, \text{ stag.}) = \Delta H_0°(trans→cis) = -170 \text{ cal/mole,}$$

$$\Delta H(cis, \text{ stag.}) = \Delta H_{\text{steric}}(cis, \text{ stag.}) + \Delta H_{\text{res}}(cis, \text{ stag.}),$$

$$\Delta H(cis, \text{ eclip.}) = \Delta H_{\text{res}}(cis, \text{ eclip.}) = -170 - 800$$

$$= -970 \text{ cal/mole.}$$

The energy change has been separated into two parts, one due to steric repulsions and the other due to the increased stability of resonance forms A and B. Since in the eclipsed configuration there are two B resonance structures, while the staggered form has only one A structure, and since the interactions are electrostatic

[12] D. R. Herschbach and L. C. Krisher, J. Chem. Phys. **28**, 728 (1959).
[13] K. S. Pitzer and N. L. Hollenberg, J. Am. Chem. Soc. **76**, 1493 (1959).
[14] N. C. Craig and E. A. Entemann, J. Am. Chem. Soc. **83**, 3047 (1961).

[15] E. B. Wilson, Jr. (unpublished work).
[16] P. S. Skell and R. G. Allen, J. Am. Chem. Soc. **80**, 5997 (1958).
[17] J. N. Butler and R. D. McAlpine, Can. J. Chem. **41**, 2487 (1963).

in nature, i.e., proportional to r^{-1}, limits can be set on $\Delta H_{res}(cis, \text{stag.})$:

$$\Delta H(cis, \text{eclip.}) \geq \Delta H_{res}(cis, \text{stag.}) \geq 1/2\Delta H_{res}(cis, \text{eclip.})$$

$$-970 \text{ cal/mole} \geq \Delta H_{res}(cis, \text{stag.}) \geq -485 \text{ cal/mole.}$$

From Eq. (1) broad limits can now be set on ΔH_{steric} (cis, stag):

$$310 \text{ cal/mole} \leq \Delta H_{steric}(cis, \text{stag.}) \leq 800 \text{ cal/mole.}$$

If the interaction between the methyl hydrogen and the $-CN$ group in this molecule is expected to obey a standard Morse-like curve, then for the $H \cdots CN$ distances in crotononitrile, the atomic separations are near the minimum of the well where both the attractive and repulsive interactions are important.

As can be seen in Table VII, five abnormally low barriers to internal rotation of methyl groups are known at this time: $cis\text{-}CH_3CH = CHF$,[4] $cis\text{-}CH_3CH = CHCl$,[18] $cis\text{-}CH_3CH = CHCH_3$,[19] $cis\text{-}CH_3CH = CHCN$,[20] and

$$cis\text{-}CH_3CH \overset{\displaystyle O}{\underset{\diagdown}{\diagup}} CHCH_3.[21]$$
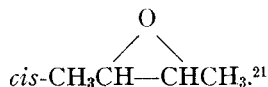
The expected lowering of V_3 in $CH_3CH_2CH_2CN$ and $CH_3CH_2CH_2F$ were not found. In particular, $CH_3CH_2CH_2F$ has two stable rotational isomers, a *trans* and a *gauche* form.[22] The barrier heights of the methyl groups in the *trans* and *gauche* forms are approximately the same though the methyl hydrogen and the fluorine atom are separated by only 2.50 Å in the *gauche* form. Propyl fluoride differs from the anomolous cases in two features: (1) the absence of a double bond, and (2) in the relative orientation of the interacting nuclei. In the five molecules with low barrier, the interacting C–H and C–X bonds are pointing towards each other. On the other hand, in $CH_3CH_2CH_2F$, the C–X and C–H bonds at the position

of closest approach are directed slightly away from each other and the interaction occurs on the bond side of the H and F nuclei.

The similar lowering of the barrier in *cis*-2, 3-epoxybutane (1.6 kcal/mole) below the value obtained in propylene oxide (2.6 kcal/mole)[23] suggests that the effect is not dependent on a double bond, but that the orientation of the interacting groups is the factor necessary for the anomoly. This effect is in agreement with a nonspherical electron distribution around the nuclei with the electron cloud extending further out on the side of the nuclei opposite to the bond.

In the past, attempts have been made to explain barriers to internal rotation by electrostatic interactions; for example, recently Silver and Wood[24] have suggested that dipole–dipole interactions may account for small variations in the barrier of similar molecules. If we choose the C–H bond moments to be 0.4 D, with H positive on methyl carbons and H negative on olefinic carbons, the barrier height variations in the fluoropropylenes will fall in the proper order, though only 50% of the variation can be accounted for. However, the additional barrier lowering in *cis*-$CH_3CH = CHCl$ relative to *cis*-$CH_3CH = CHF$ is not explained. Likewise, the small changes in barrier heights in the haloethanes or the acetyl halides are not explained by the above sign choice for the C–H bond moment.

It is worthwhile to re-emphasize that the convergence of the multipole expansion is questionable at such short distances: we are dealing with bonds of 1.5 Å length interacting at distances of 2.5 Å.

ACKNOWLEDGMENTS

[18] R. A. Beaudet, J. Chem. Phys. **37**, 2398 (1962).
[19] T. N. Sarachmann, Ohio State Symposium on Molecular Structure and Spectroscopy, Columbus, Ohio, 1963 (V_3=0.750 kcal).
[20] R. A. Beaudet, J. Chem. Phys. **38**, 2548 (1963).
[21] M. L. Sage, J. Chem. Phys. **35**, 142 (1961).
[22] E. Hirota, J. Chem. Phys. **37**, 283 (1962).

[23] J. D. Swalen and D. R. Herschbach, J. Chem. Phys. **27**, 100 (1957).
[24] H. G. Silver and J. L. Wood, Trans. Faraday Soc. **59**, 588 (1963).